


RESEARCH

Open Access



The added value of relative amide proton transfer (rAPT) to advanced multiparametric MR imaging for brain glioma characterization

Mai A. Mostafa^{1,4*} , Pasant M. Abo-Elhoda¹, Ahmed S. Abdelrahman¹, Ahmed M. Elzoghby², Manal M. Elmahdy³ and Yasser A. Abbas¹

Abstract

Background Differentiation between the grades of brain gliomas is a crucial step in the management of patients. The gold standard technique for grading is biopsy but MR imaging may play a more substantial role as a non-invasive method by using promising molecular sequences. Our purpose was to assess the added value of the relative amide proton transfer signal [rAPT] to advanced multiparametric MRI protocol.

Methods We enrolled a pathologically confirmed 102 patients with low-grade glioma [$n=38$] and high-grade glioma [$n=64$] who underwent advanced multiparametric MRI protocol on the same scanner. The protocol included anatomic, diffusion, MRS, and perfusion sequences. The newly added sequence was Amide proton transfer. The rAPT values of all lesions were investigated by two neuroradiologists to assess the inter-rater agreement of using interclass correlation coefficient [ICC]. HGGs demonstrated significantly higher mean values of relative cerebral blood volume (rCBV), choline to creatine ratio (Cho/cr), and rAPT with lower Apparent diffusion coefficient (ADC) values compared to LGGs. ROC analyses revealed medium to high diagnostic performance with an AUC of 0.941 for rAPT, 0.907 for mean ADC, and 0.906 for rCBV. Discriminant function analysis of two models, the first one included mean ADC, rCBV, and Cho/Cr, while in the second Model, we added rAPT to them. Model two demonstrated higher accuracy and a significant difference in the AUC after adding the rAPT. The inter-rater agreement was reasonable (ICC 0.61).

Conclusions rAPT adds significant value to multiparametric MRI for distinguishing LGG from HGG.

Keywords Brain glioma, MRI brain, Advanced MRI brain, APT, Relative APT

Background

Gliomas are the most common primary tumors of the central nervous system [1]. Differentiating low-grade glioma [LGG] from high-grade glioma [HGG] is crucial for prognosis and management [2].

Biopsy with histopathology is the current gold standard examination for discriminating gliomas. However, the histopathological result depends on biopsy conditions which have drawbacks, including being invasive, the intratumoral histological heterogeneity and edema influencing it, and the possibility of exhibiting sampling errors, which may all affect the actual tumor grade [3].

*Correspondence:

Mai A. Mostafa

mai.ahmed@med.asu.edu.eg

¹ Department of Radiodiagnosis, El Demerdash Hospital, Ain Shams University, Cairo, Egypt

² Faculty of medicine, Ain Shams University, Cairo, Egypt

³ Department of Pathology, El Demerdash Hospital, Ain Shams University, Cairo, Egypt

⁴ Radiology Department, El Demerdash Hospital, Ain Shams University, Cairo, Egypt

Magnetic resonance imaging is usually done preoperatively for diagnosis as a non-invasive procedure [4]. The pattern of enhancement is different between HGGs and LGGs, where the former shows mild enhancement. However, approximately 14–45% of HGGs show no enhancement, whereas about 20% of enhanced gliomas were histologically proven to be LGGs, as the degree of enhancement might be caused by disruption of the blood–brain barrier rather than neovascularization. Therefore, the accurate grading of gliomas using traditional MRI is still challenging [5, 6].

Dynamic contrast-enhanced MRI [DCE], perfusion, susceptibility-weighted imaging, diffusion-weighted imaging [DWI], MR spectroscopy [MRS], and intravoxel incoherent motion are advanced MRI techniques that are used for glioma grading [7, 8]. Despite being useful, DCE MRI relies on gadolinium contrast, but few complications were reported as nephrogenic systemic fibrosis may increase in patients with impaired renal function or acclimation of contrast in the brain of a normal population if there are repeated administrations [9].

In MRS, increases in choline [Cho]-containing compounds are markers for accelerated cell proliferation, as they reflect increased protein expression and proteolysis [7, 8]. Nevertheless, its accuracy in differentiation is erratic because it is operator-dependent on choosing a voxel place, and this technique does not involve the whole tumor [10]. So, in our advanced protocol, we added a new technique which is Amide proton transfer [APT].

The Amide proton transfer [APT] is a promising molecular-based MRI technique as previous studies have indicated that APT signals could be used to assess brain tumors due to overexpressed mobile protein and peptide concentrations [11–13]. APT is a non-invasive technique that does not require contrast administration. It could be used as a substitute for contrast-based MRI, especially in patients with contraindications for a contrast agent. APT also has the practical advantage that acquisition can be immediately repeated in case of suboptimal image quality, which is not the case with perfusion studies [14].

Several studies showed that HGGs had higher APT signal intensity than LGGs [15–17], but a limited number of studies assessed the relative APT signal [rAPT] of brain tumor versus normal brain tissue but with no clear cutoff value [18, 19].

In this study, we evaluated the added value of rAPT to multiparametric MRI in assessing brain gliomas.

Methods

This prospective cohort study was approved by our institution's ethical committee -FWA 000017585- FMASU R210/2021. Our inclusion criteria were adult patients ranging from 18 to 83 years old, undergoing multiparametric MR imaging and APT in the same scanner. The HGGs or LGGs are confirmed by histopathology. The excluded patients were those who had motion artifacts, impaired renal functions, or lack of final diagnosis.

The preoperative MR imaging data of 135 patients with gliomas were identified between December 2020 and April 2022. Out of these patients, ten patients were excluded due to motion artifacts on imaging, thirteen patients were excluded due to impaired renal functions, and ten others were excluded due to lack of final diagnosis.

The histopathologic diagnosis was determined by histopathology with biopsy specimens or resections by one neuropathologist, who was blinded to the imaging findings. The patients were divided into two groups including low-grade [1 and 2] and high-grade [3 and 4] gliomas based on the pathological results.

Studies were performed on a 3.0-T clinical scanner [Magnetom Skyra, Siemens]. The detailed imaging parameters for advanced multiparametric sequences including APT are shown in Table 1. APT imaging was acquired using the two-dimensional single-shot fast spin echo planner imaging [EPI] For the APT quantification, after water frequency-shift correction, magnetization transfer component, and the APT [$\Delta\omega = 3.5$ ppm] component, asymmetrical MT ratio [MTR_{asym}] analysis was performed according to previous studies. The DWI was performed in the axial plane with a single-shot spin-echo

Table 1 Imaging parameters

	APT	DWI	T1	T2	FLAIR	Post-contrast T1 WI	Perfusion
TR	4–5 ms	5100 ms	5000 ms	7120 ms	9000 ms	2220 ms	1650 ms
TE	2 ms	64 ms	11 ms	119 ms	113 ms	8.5 ms	30 ms
FOV	220 × 813 mm ²	220 × 100 mm ²	240 × 78 mm ²	240 × 81 mm ²	240 × 84 mm ²	220 × 84 mm ²	240 × 100 mm ²
Slice thickness	5 mm	4 mm	4–5 mm	3 mm	3 mm	4–5 mm	4mm
Scan time	3 min and 7 s	26 s	1min and 57s	1min and 6 s	3 min	2 min	10 min
Matrix	100 × 100	160 × 100	256 × 75	284 × 80	256 × 80	256 × 75	128 × 100

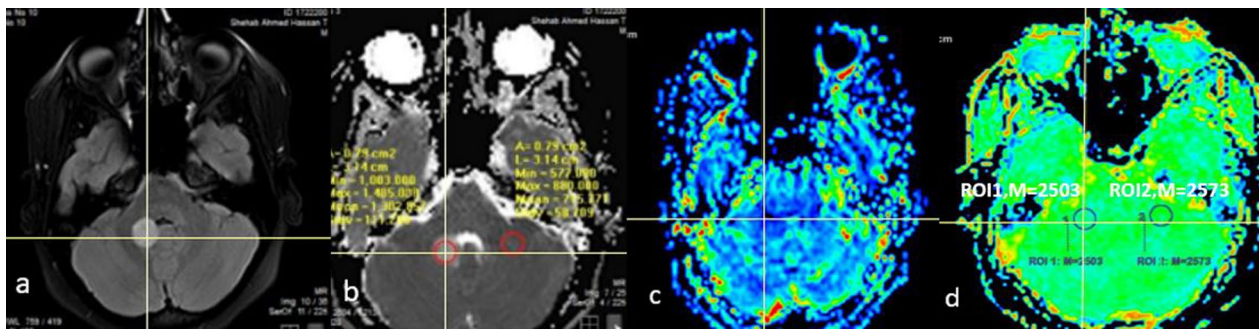


Fig. 1 A 44-year-old female patient presented with vertigo and pathologically proved low-grade glioma at the right cerebellar peduncle with MR images as follows: **a** Axial FLAIR image shows a well-defined high signal intensity lesion within the right cerebellar peduncle with no surrounding edema, **b** ADC map shows no true diffusion restriction within the lesion, **c** CVB map shows iso- to hypoperfused lesion, and **d**-APT map also shows iso-intensity of the lesion compared to contralateral side with $rAPT=0.97$ (Note that the interlink lines are used to draw ROIs)

planar imaging sequence of b values; 0 and 1000 [s/mm²]. The apparent diffusion coefficient (ADC) was calculated by mono-exponential fitting with the pair of b-values.

The acquired data were transferred from the scanner to a workstation for analysis and postprocessing. Region-of-interests (ROIs) for HGG were manually drawn on post-contrast images and matched by the interlink lines to FLAIR, ADC, cerebral blood volume (CBV), and APT maps. For LGG and or non-enhancing lesions ROIs were manually drawn on FLAIR and matched to post-contrast images, ADC, cerebral blood volume (CBV), and APT map (Fig. 1). Two neuroradiologists experts of 10- and 40 years' experience calculated the $rAPT$ independently by dividing the mean value of the APT signal intensity of the lesion by the mean APT value of normal white matter on the contralateral side. Readers were aware that they must avoid necrotic regions, hemorrhage, obvious artifacts, or signals from a blood vessel, during drawing the ROI as this can cause substantial reading artifacts. We calculated the relative CBV values ($rCBV$) by normalization to the contralateral normal-appearing gray matter.

Statistical analysis

- The sample size was calculated using MedCalc Statistical Software version 15.8 (MedCalc Software bvba, Ostend, Belgium; <https://www.medcalc.org>; 2015), setting the type-1 error (α) at 0.05 and the power ($1-\beta$) at 0.8. Results from a previous study (C.su et al., 2017) reported an AUC to differentiate between LGG and HGG of 0.791. Based on these values the calculated sample size was at least 18 high-grade and at least eighteen low-grade cases achieving an AUC of 0.79 with a 95% confidence interval of 0.3.
- Data were analyzed using Statistical Package for Social Science [IBM Corp. Released 2017. IBM SPSS

Statistics for Windows, Version 25.0. Armonk, NY: IBM Corp.]. Quantitative parametric variables were described using the range, mean, and standard deviation. Qualitative variables were described using numbers and percentages. The first analysis was done using an independent sample t-test that compared the mean of continuous variables. P value < 0.05 was considered statistically significant for all statistical methods. Receiver operator characteristic [ROC] curve analysis was then performed to determine the optimal cutoff value of variables that passed the first analysis.

- A discriminant function analysis [DFA] was then used for variables that achieved significant results in this second analysis [p value < 0.05], and the variables were classified into two models: Model 1 multiparametric study which included ADC, MRS, CH/Cr, and $rCBV$, and model 2 multiparametric study which included $rAPT$, ADC, MRS, CH/Cr, and $rCBV$. The diagnostic performance of the categorical variable was performed using cross-tabulation. The sensitivity, specificity, and accuracy were then calculated.
- The eigenvalue was calculated to determine the efficiency of all variables in the model in predicting brain glioma grading. Standardized DFA coefficients were also calculated to demonstrate the unique contribution of each predictor variable to the function. Paired-Sample Area Difference under the ROC Curves was conducted to determine the difference between the AUC of both models.
- We determined the inter-rater agreement using the intra-class correlation coefficient (ICC) (20). ICC scores below 0.4 were considered as poor agreement, 0.4–0.6 as reasonable, 0.6–0.7 as good, and 0.7–1 as excellent [20].

Results

The total number of patients was 102 [61 males and forty-one females], 38 of them had LGGs and 64 had HGGs. The mean age of patients was 41.7 years, [range 18–83 years]. An observation was noted that the incidence of HGG increased with age. The rest of the demographic and general characteristics of patients are described in Table 2.

Hemorrhage, peritumoral edema, central necrosis, and ring contrast enhancement were analyzed in both HGGs and LGGs on conventional and post-contrast images using an independent t-test. Hemorrhage was observed in 45.3% of HGGs and 5.3% of LGGs. About 67.2% of HGGs and 26.3% of LGGs showed peritumoral edema. We observed central necrosis in 62.5% of HGGs and 26% of LGGs. Ring post-contrast enhancement was seen in 54.7% of HGGs and 7.9% of LGGs.

To assess the reliability and consistency of rAPT measurements between the two readers, Inter-rater agreement was evaluated using the intra-class correlation coefficient (ICC) which revealed a reasonable value of 0.61.

Using an independent sample t-test showed significantly higher mean values of rCBV, Cho/cr, and rAPT (Figs. 2, 3), as well as lower ADC values in HGGs compared to LGG tumors. The mean value of rAPT in HGGs was 2.12 ± 0.11 while in LGGs was 1.46 ± 0.27 . HGG mean value of rCBV was 5.38 ± 2.99 while the LGGs were 2.12 ± 0.49 . The mean value of Cho/cr in HGGs was 3.59 ± 3.31 while in LGGs was 1.65 ± 0.60 . The mean value of ADC in HGGs was 0.97 ± 0.17 while in LGGs was 1.39 ± 0.26 .

The ROC (Table 3) was used to analyze the discriminatory abilities of rAPT, mean ADC, rCBV, and Cho/cr values which revealed medium to high diagnostic performance of all parameters. The area under the curve [AUC] was 0.941 for rAPT, 0.907 for mean ADC, and 0.906 for rCBV with cutoff values of 1.315, 1.12, and 2.36, respectively.

To assess the added value of rAPT to multiparametric MRI, we used the discriminant function analysis [DFA] test between two models, where the first one included the multiparametric MRI without rAPT, while in the second one rAPT was added to them. As demonstrated in (Table 4). There was an increase in the eigenvalue of the second model after adding the rAPT, with an increase in diagnostic performance from 83.33 to 94.11 (Table 5). Moreover, Table 6 illustrates the higher accuracy and significant increase in the AUC of the second model.

Discussion

APT imaging is a novel MRI technique that provides molecular information predominantly based on the amide protons in cellular proteins and peptides in the intracellular and extracellular spaces [15]. Higher peptide and protein concentrations usually result from higher cell density in HGGs [16, 17]. Kang et al. [15], Schön et al. [16], Sakata et al. [17], and Sotirios et al. [11] studies showed that HGGs had higher APT signals than LGGs. Recent limited studies assessed the relative APT signal of primary and secondary brain tumors compared to normal brain tissue but neither of them sets a clear cutoff value of rAPT for HGGs or LGGs [18, 19, 21].

Table 2 Demographic and general characteristics of brain tumors

	All tumors [102]	Low grade [38]	High grade [64]	P value
Age [mean ± SD]	41.7 ± 19.4 [18–83]	33.7 ± 16.1 [11–75]	45.3 ± 19.5 [10–83]	0.003*
Sex				0.471
Male	61 [59.8%]	21 [55.3%]	40 [62.5%]	
Female	41 [40.2%]	17 [44.7%]	24 [37.5%]	
Location				0.064
Lobar	71 [69.6%]	22 [57.9%]	49 [76.6%]	
BS	12 [11.8%]	4 [10.5%]	8 [12.5%]	
BG	9 [8.8%]	4 [10.5%]	5 [7.8%]	
Thalamus	2 [2%]	1 [2.6%]	1 [1.6%]	
Hypothalamus	2 [2%]	2 [5.3%]	0	
Cerebellum	6 [5.9%]	5 [13.2%]	1 [1.6%]	
Multiplicity				0.153
Single	81 [79.4%]	33 [86.8%]	48 [75%]	
Multiple	21 [20.6%]	5 [13.2%]	16 [25%]	

*Significant

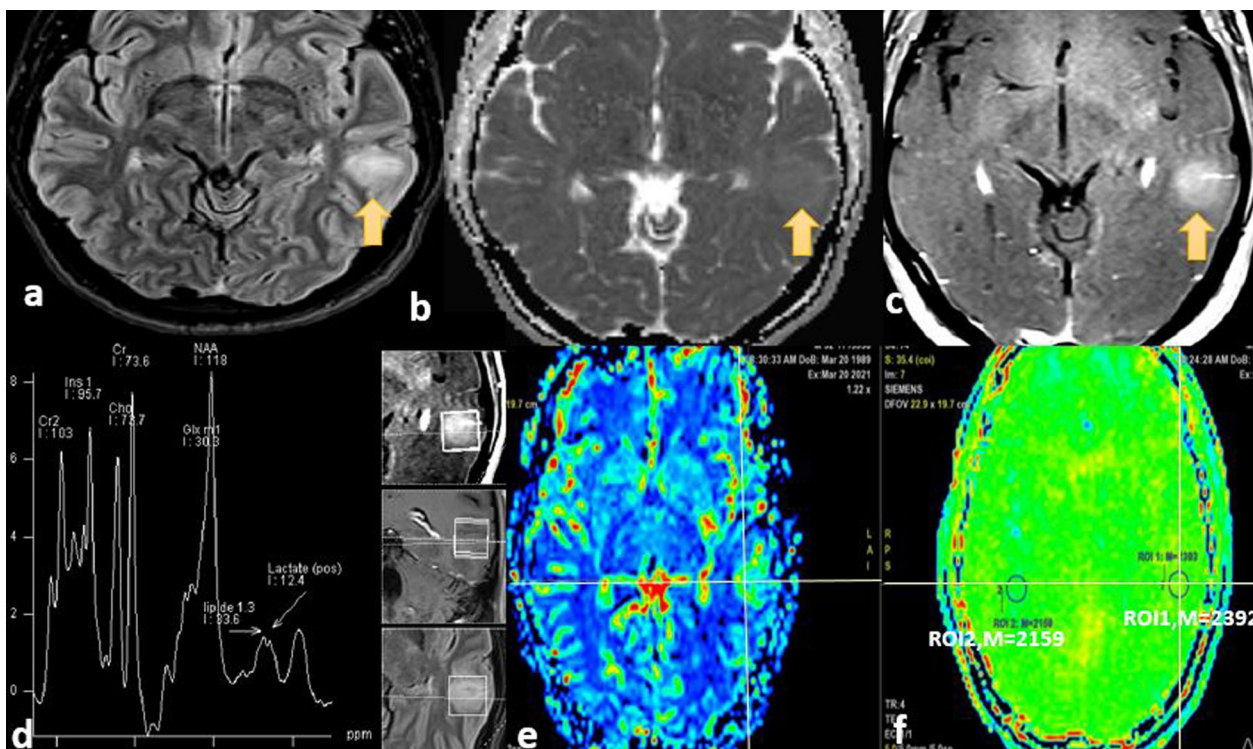


Fig. 2 A 39-year-old male patient presented with a headache and was pathologically proven low-grade glioma at the left temporal lobe with MR images as follows: **a** FLAIR shows the high signal intensity of the focal lesion (arrow), **b** ADC map shows no true diffusion restriction of the lesion (arrow), **c** axial post-contrast image shows homogeneous faint post-contrast enhancement (arrow), **d** MRS shows low Cho/cr ratio, **e**- CVB map shows hypoperfusion of the lesion, **f**-APT map shows iso intense signal of the lesion with rAPT= 1.1

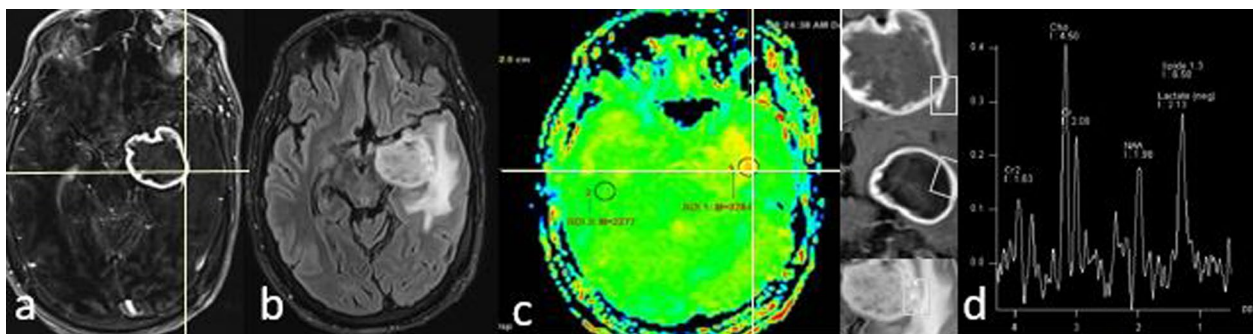


Fig. 3 A 56-year-old female patient presented with a headache and was pathologically proven left temporal high-grade glioma with MR images as follows: **a** axial post gadolinium T1 WI shows marginal enhancement of the lesion, **b** Axial FLAIR images show a rather well-defined hyperintense lesion with surrounding vasogenic edema, **c** APT image shows a high-intense signal of the lesion compared to the contralateral normal white matter with rAPT= 1.43, **d** MRS shows high Cho/cr ratio

Our primary aim was to assess the added value of relative APT [rAPT] to multiparametric MRI brain to distinguish LGGs and HGGs so we first assessed the inter-reader agreement using the intra-class correlation coefficient. There was a reasonable inter-rater agreement of rAPT values (ICC=0.61) that can be explained by the difference in the experience of our readers.

As regards the rAPT values our results showed that HGGs had significantly higher rAPT than LGGs. This was consistent with the results of the previous two studies which were done recently to assess APT signals in different brain tumors versus normal white matter [18, 19].

Then we assessed the diagnostic performance of rAPT using the ROC which revealed medium to high

Table 3 ROC shows Cut off value of rAPT, ADC, rCBV and Cho/cr for predicting high-grade tumor

	AUC	95% CI	P value	Cut off	TP	TN	FP	FN	Sen	Spe	PPV	NPV	Acc
rAPT	0.941	0.895–0.986	<0.001*	1.315 [#]	61	32	6	3	95.3	84.2	91	91.4	91.2
ADC mean	0.907	0.853–0.961	<0.001*	1.125 ⁺	46	33	5	18	71.9	86.8	90.2	64.7	77.5
rCBV/Tumor	0.906	0.580–0.961	<0.001*	2.365 [#]	60	27	11	4	93.8	71.1	84.5	87.1	85.3
Cho/Cr	0.797	0.712–0.882	<0.001*	1.69 [#]	48	23	15	16	75	60.5	76.2	59	69.6

Total number of brain tumors with edema is 53 brain SOL

* indicates significant

⁺ indicates equal or less than cut off value

[#] indicates equal or greater than cut off value

Table 4 Discriminant function analysis [DFA] between two multiparametric models

	Model 1	Model 2
Eigenvalue	0.727	0.761
Standardized DFA coefficients		
ADC	0.760	0.656
rCBV	0.349	0.250
MRS Cho/Cr	0.269	0.271
rAPT		0.437

diagnostic performance of rAPT with AUC of 941 and cutoff value of 1.31, achieving a sensitivity of 95% and specificity of 84%. The earlier studies did not set a cut-off value of rAPT to differentiate grades of glioma, but one of them compared the APT signal of glioblastoma to normal brain tissue, achieving 100% sensitivity and 80% specificity with an AUC of 960 [18].

Currently, different imaging techniques are applied to differentiate HGGs and LGGs, such as DWI, rCVB, and MRS, but many authors investigated the added value of APT as Choi et al. [22] study revealed that discrimination abilities of the APT, ADC, and rCBV values were not significantly different but did not investigate the rAPT.

Our results proved that rAPT had a comparable ability to predict tumor grade as rCBV and had better discrimination ability than the ADC, which was also consistent with Lingl et al. [18] differentiation of glioblastoma from the normal brain tissue. Durmo et al. [19] study demonstrated also that APT was a better predictor than ADC in differentiating LGGs from HGGs. This could

Table 6 Difference between AUC of model 1 and model 2

	AUC	95% CI	z	P value
Model 1	0.819	0.727–0.911	–3.383	0.001
Model 2	0.932	0.869–0.994		

be explained by the overexpression of various proteins in the extracellular matrix in high-grade glioma and in turn, increase the fluid mobility within the extracellular environment. Thus, causes higher ADC in the enhancing area than those with lower ADC, but an increase in the mobile peptides will increase APT-related signal [23, 24].

In addition, rAPT showed comparable diagnostic capability for grading brain tumors as Cho/cr ratios on MRS. Sakata et al. [25] study also concluded that MRS and APT imaging had a comparable diagnostic capability for grading brain tumors.

Choi et al. [22] investigated the added value of APT when used with ADC which showed significant improvement in the discrimination ability of brain glioma compared to the ADC alone with AUC 910 versus 888.

To date, no studies investigated the added value of rAPT to multiparametric MRI brain protocol including rCVB, ADC, and MRS. We used the DFA, and we observed a significant increase in the diagnostic performance of the multiparametric protocol when the rAPT was added, increasing the AUC from 819 to 932.

The strength of our study was achieved by enrolling a large sample size [more than one hundred], Also we are suggesting a new parameter called rAPT which was not investigated in depth in previous studies and

Table 5 Diagnostic performance of discriminant function analysis between two multiparametric models

	TP	TN	FP	FN	Sen	Spe	PPV	NPV	Acc
Model 1	56	29	9	8	87.5	76.3	86.2	78.4	83.33
Model 2	62	34	4	2	96.9	89.5	93.9	94.4	94.11

Model 1 = ADC, MRS, CH/Cr, and rCBV

Model 2 = rAPT, ADC, MRS, CH/Cr and rCBV

has comparable results to other advanced techniques and can be used without contrast injection. Nevertheless, we also had limitations. First, it was a single-centered study. Thus, conducting multi-centric studies with larger data sets is required to validate the results. Moreover, a manual ROI-based approach was performed for analysis in our research.

Conclusions

In conclusion, rAPT is a useful non-invasive imaging biomarker that significantly increases the diagnostic performance of the multiparametric protocol. We believe that the rAPT techniques can be a valuable tool if a patient refuses a contrast injection or has contraindications for a contrast agent. Furthermore, it can be used in research to differentiate post-treatment changes in glioma versus residual tumoral tissue.

Abbreviations

APT	Amide proton transfer
rCBV	Relative cerebral blood volume
Cho/cr	Choline/creatine
Cho/Naa	Choline/N-acetyl aspartate
DCE	Dynamic contrast-enhanced
DFA	Discriminant function analysis
ICC	Intra-class correlation coefficient
IDH	Isocitrate dehydrogenase
IVIM	Intravoxel incoherent motion
HGG	High-grade glioma
LGG	Low-grade glioma
rAPT	Relative amide proton transfer
ROC	Receiver operating characteristic
WHO	World health organization

Acknowledgements

Not applicable.

Author contributions

MAM is Corresponding author, her role was collecting and interpreting data as well as scientific writing of most of the article. PMA is co-author: her role was collecting the data and writing the introduction. ASA is co-author: his main role was calculating the statistics. AME is co-author: his role was collecting and archiving the data. MME is co-author: her main role was Histopathological assessment. YAA is co-author: the core idea belongs to him and his main role was interpreting the data. All authors read and approved the final manuscript.

Funding

No financial interests directly or indirectly related to the work submitted for publication.

Availability of data and materials

The datasets used and/or analyzed during the current study are available from the corresponding author on reasonable request.

Declarations

Ethics approval and consent to participate

Study was approved by our institution's ethical committee -FWA 000017585-FMASU R210/2021.

Consent for publication

Not applicable.

Competing interests

The authors declare that they have no conflict of interest.

Received: 6 July 2023 Accepted: 2 September 2023

Published online: 27 October 2023

References

- Anaraki A, Ayati M, Kazemi F (2019) Magnetic resonance imaging-based brain tumor grades classification and grading via convolutional neural networks and genetic algorithms. *Biocybern Biomed Eng* 39(1):63–74. <https://doi.org/10.1016/j.bbe.2018.10.004>
- Clarke J, Butowski N, Chang S (2010) Recent advances in therapy for glioblastoma. *Arch Neurol* 67(3):279–283. <https://doi.org/10.1001/archneurol.2010.5>
- Togao O, Yoshiura T, Keupp J et al (2014) Amide proton transfer imaging of adult diffuse gliomas: correlation with histopathological grades. *Neuro Oncol* 16(3):441–448. <https://doi.org/10.1093/neuonc/not158>
- Sawhani V, Patel M, Davies N et al (2020) Multiparametric MRI: a practical approach and pictorial review of a useful tool in the evaluation of brain tumors and tumor-like lesions. *Insights Imaging* 11:84. <https://doi.org/10.1186/s13244-020-00888-1>
- Fan G, Deng Q, Wu Z et al (2006) The usefulness of diffusion/perfusion-weighted MRI in patients with non-enhancing supratentorial brain gliomas: a valuable tool to predict tumor grading? *Br J Radiol* 79(944):652–658. <https://doi.org/10.1259/bjr/25349497>
- McKnight T, Lamborn K, Love T et al (2007) Correlation of magnetic resonance spectroscopic and growth characteristics within grades II and III gliomas. *J Neurosurg* 106(4):660–666. <https://doi.org/10.3171/jns.2007.106.4.660>
- Howe F, Barton S, Cudlip S et al (2003) Metabolic profiles of human brain tumors using quantitative in vivo 1H magnetic resonance spectroscopy. *Magn Reson Med* 49(2):223–232. <https://doi.org/10.1002/mrm.10367>
- Shimizu H, Kumabe T, Shirane R et al (2000) Correlation between choline level measured by proton MR spectroscopy and Ki-67 labeling index in gliomas. *AJNR Am J Neuroradiol* 21(4):659–665
- Gulani V, Calamante F, Shellock FG et al (2017) Gadolinium deposition in the brain: summary of evidence and recommendations. *Lancet Neurol* 16(7):564–570. [https://doi.org/10.1016/S1474-4422\(17\)30158-8](https://doi.org/10.1016/S1474-4422(17)30158-8)
- Omuro A, Leite C, Mokhtari K et al (2006) Pitfalls in the diagnosis of brain tumors. *Lancet Neurol* 5(11):937–948. [https://doi.org/10.1016/S1474-4422\(06\)70597-X](https://doi.org/10.1016/S1474-4422(06)70597-X)
- Sotiriou B, Demetriou E, Topriceanu CC et al (2020) The role of APT imaging in gliomas grading: a systematic review and meta-analysis. *Eur J Radiol* 133:109353. <https://doi.org/10.1016/j.ejrad.2020.109353>
- Xie T, Chen X, Fang J et al (2018) Textural features of dynamic contrast-enhanced MRI derived model-free and model-based parameter maps in glioma grading. *J Magn Reson Imaging* 47(4):1099–1111. <https://doi.org/10.1002/jmri.25835>
- Zhou J, van Zijl PCM (2006) Chemical exchange saturation transfer imaging and spectroscopy. *Prog Nuclear Magn Reson Spectrosc* 48(2–3):109–136. <https://doi.org/10.1016/j.pnmrs.2006.01.001>
- Frismose A, Markovic L, Nguyen N et al (2022) Amide proton transfer-weighted MRI in the clinical setting—correlation with dynamic susceptibility contrast perfusion in the post-treatment imaging of adult glioma patients at 3T. *Radiography* 28(1):95–101. <https://doi.org/10.1016/j.radi.2021.08.006>
- Kang X, Xi Y, Liu T et al (2020) Grading of Glioma: combined diagnostic value of amide proton transfer weighted, arterial spin labeling, and diffusion-weighted magnetic resonance imaging. *BMC Med Imaging* 20:1. <https://doi.org/10.1186/s12880-020-00450-x>
- Schön S, Cabello J, Liesche-Starnecker F et al (2020) Imaging glioma biology: spatial comparison of amino acid PET, amide proton transfer, and perfusion-weighted MRI in newly diagnosed gliomas. *Eur J Nucl Med Mol Imaging* 47(6):1468–1475. <https://doi.org/10.1007/s00259-019-04677-x>
- Sakata A, Okada T, Yamamoto A et al (2015) Grading glial tumors with amide proton transfer MR imaging: different analytical approaches. *J Neurooncol* 122:339–348. <https://doi.org/10.1007/s11060-014-1715-8>

18. Lingl J, Wunderlich A, Goerke S et al (2022) The Value of APTw CEST MRI in routine clinical assessment of human brain tumor patients at 3T. *Diagnostics* 12(2):490. <https://doi.org/10.3390/diagnostics12020490>
19. Durmo F, Rydhög A, Testud F et al (2020) Assessment of Amide proton transfer weighted (APTw) MRI for pre-surgical prediction of final diagnosis in gliomas. *PLoS ONE*. <https://doi.org/10.1371/journal.pone.0244003>
20. Liljequist D, Elfving B, Roaldsen KS (2019) Intraclass correlation—a discussion and demonstration of basic features. *PLoS ONE* 14(7):e0219854. <https://doi.org/10.1371/journal.pone.0219854>
21. Yu H, Lou H, Zou T et al (2017) Applying protein-based amide proton transfer MR imaging to distinguish solitary brain metastases from glioblastoma. *Eur Radiol* 27(11):4516–4524. <https://doi.org/10.1007/s00330-017-4867-z>
22. Choi Y, Ahn S, Lee S et al (2017) Amide proton transfer imaging to discriminate between low- and high-grade gliomas: added value to apparent diffusion coefficient and relative cerebral blood volume. *Eur Radiol* 27(8):3181–3189. <https://doi.org/10.1007/s00330-017-4732-0>
23. Pope W, Mirsadraei L, Lai A et al (2012) Differential gene expression in glioblastoma defined by ADC histogram analysis: relationship to extracellular matrix molecules and survival. *AJNR Am J Neuroradiol* 33(6):1059–1064. <https://doi.org/10.3174/ajnr.A2917>
24. Nakajo M, Bohara M, Kamimura K et al (2021) Correlation between amide proton transfer-related signal intensity, diffusion, and perfusion magnetic resonance imaging parameters in high-grade glioma. *Sci Rep* 11(1):11223. <https://doi.org/10.1038/s41598-021-90841-z>
25. Sakata A, Fushimi Y, Okada T et al (2017) Diagnostic performance between contrast enhancement, proton MR spectroscopy, and amide proton transfer imaging in patients with brain tumors. *J Magn Reson Imaging* 46(3):732–739. <https://doi.org/10.1002/jmri.25597>

Publisher's Note

Springer Nature remains neutral with regard to jurisdictional claims in published maps and institutional affiliations.

Submit your manuscript to a SpringerOpen[®] journal and benefit from:

- Convenient online submission
- Rigorous peer review
- Open access: articles freely available online
- High visibility within the field
- Retaining the copyright to your article

Submit your next manuscript at ► [springeropen.com](https://www.springeropen.com)
